JOURNAL OF FOREST SCIENCE, *63*, 2017 (8): 355–362

doi: 10.17221/15/2017-JFS

Forest density and orchard classification in Hyrcanian forests of Iran using Landsat 8 data

Khosrow MIRAKHORLOU, Reza AKHAVAN*

Research Institute of Forests and Rangelands, Agricultural Research, Education and Extension Organization (AREEO), Tehran, Iran

**Corresponding author: khosrowm40@gmail.com*

Abstract

Mirakhorlou K., Akhavan R. (2017): Forest density and orchard classification in Hyrcanian forests of Iran using Landsat 8 data. J. For. Sci., 63: 355–362.

Satellite-based remote sensing is of crucial importance to provide timely and continuous thematic maps for practical forestry tasks. There is currently no existing remote sensing-based, large-scale inventory of canopy cover classes (and also adjacent orchards) on the full range of Hyrcanian forests. We used the freely available and large-scale coverage of Landsat 8 imagery acquired in 2014 to classify three forest density classes as well as non-forest and orchards. The supervised classification and support vector machine classifier were selected based on a pre-classification of three representative pilot regions. Classified final maps were validated by means of a two-stage sampling and 1,852 field samples. The total areas of the dense, semi-dense, sparse forests and orchards were 45, 36, 19 and 1.9% of the total studied area, respectively. The overall accuracy and Kappa coefficient of classified maps were 94.8 and 90%, respectively. The methodology introduced to map forest cover in Hyrcanian forests is concluded to enable providing a high quality forest database for further research, planning and management.

Keywords: canopy cover; Caspian forests; satellite data; supervised classification; support vector machines; two-stage sampling

Hyrcanian forests are located along the southern part of the Caspian Sea and the north-facing aspects of Elborz Mountains in the north of Iran, and embrace natural, mixed hardwood and generally uneven-aged deciduous forests (Akhavan et al. 2012). They are considered as remnants of the Tertiary era, consist of more than 80 woody species and mainly include five main vegetation communities of *Querco-Buxetum*, *Querco-Carpinetum*, *Parrotio-Carpinetum*, *Fagetum hyrcanum*, and *Carpinetum orientale*. Owing to the necessity of management, protection and restoration of these forests, timely spatial information on stand density and distribution is a prerequisity for forest management programs.

Remotely sensed information provided by satellite missions can provide this information in a continuous manner, particularly in combination with geo-located field-based surveys. The freely available 8 multispectral sensors from the Landsat 8 Operational Land Imager (OLI) sensor (185 km wide swath and 16 day temporal resolution) are assumed to present valuable opportunities for thematic mapping of forestry attributes (e.g. density and land covers). Moreover, the continuous coverage of Landsat legacy archive makes it an outstanding key primary data source for regional analyses, particularly in resource-limited and logistically inaccessible areas (Dube, Mutanga 2015).

Landsat data have been numerously applied to distinguish land cover over the past decades, with the recent examples being Mirakhorlou (2003), Mirakhorlou and Akhavan (2008), Saadat et

Supported by the Department of Environment of Iran, Project No. 6414.

al. (2011), Salman Mahini et al. (2012), Tazeh et al. (2014), and Qin et al. (2015). The classifiers include supervised parametric (e.g. maximum likelihood – ML) and non-parametric machine learning (neural networks – NN and support vector machines – SVM) approaches applied for classification, for which also comparative studies exist (Szuster et al. 2011). The ML classifier is one of the most efficient parametric methods for image classification (Jensen 2005), whereas approaches such as NN and SVM are non-parametric and principally do not assume normal distribution within the data (Lu, Weng 2007; Dixon, Candade 2008). However, recent comparative studies have suggested that the SVM can provide appropriate results for classification of Landsat imagery compared to traditional remote sensing classifiers such as ML, *k*-nearest neighbour and approximate nearest neighbour (Huang et al. 2002; Melganni, Bruzzone 2004; Pal, Mather 2005; Mountrakis et al. 2011; Yang, Ross 2012).

The objectives of this study were: (*i*) separation of orchards located at the border of or inside the forest, (*ii*) determination of forest density classes, (*iii*) selection of the most appropriate classifier for orchard detection and forest density classification using Landsat 8 OLI data in the large-scale mapping of Hyrcanian forests of northern Iran.

MATERIAL AND METHODS

Study area. The study area encompassed the entire Hyrcanian forests in the north of Iran, extended between 36° to 38°N and 48° to 56°E. These forests horizontally expand 800 km in an east-to-west direction and vertically from coastal plain up to 2,700 m a.s.l. tree line where convert to mountainous rangelands. An area of about 6 million ha was considered, comprising 93 standard sheets of 1:50,000 scaled topographic maps provided by the National Cartographic Centre – NCC (Fig. 1).

Data and pre-processing. Nine full Landsat 8 OLI scenes from June, August and October 2014 were applied. Image pre-processing and classification were accomplished using ERDAS Imagine software (Version 2014) (Intergraph 2013). Data management, spatial analysis and validation were done using ArcGIS software, ArcMap (Version 10.2, 2013). The data were orthofied and geometrically corrected in the NCC using both topographic maps of 1:25,000 scale and ASTER Global DEM (Version 2, 2011), its scene (60 × 60 km) having vertical root mean square errors (RMSEs) accuracies generally between 10 and 25 m and pixel size 25 m to improve the precision of the images. Coordinate systems WGS1984, 39 and 40 Zones were used for georeferencing in the study area. 25 ground control points (GCPs) were selected on roads and rivers vector layers in each scene. Furthermore, a polynomial nonparametric method was used for the removal of inappropriate GCPs, which resulted in the RMSEs of 0.18, 0.15, 0.17, 0.20, 0.19, 0.16, 0.19 and 0.18 pixels for the remaining 21, 20, 22, 23, 21, 22, 21 and 20 GCPs in the 8 scenes, respectively. Atmospheric correction was not necessary because the image was quite clear within the study area.

Experimental design. Many factors affect the performance of a classifier, including the selection of training and testing data samples as well as input variables (Foody et al. 1995). Because the impact of testing data selection on accuracy assessment has been investigated in many works (e.g. Stehman 1992), only the selection of training sample and the input variable were considered in this study. In order to avoid biases in the confidence level of accuracy estimates due to inappropriately sampled testing data (Dicks, Lo 1990), the accuracy measure of

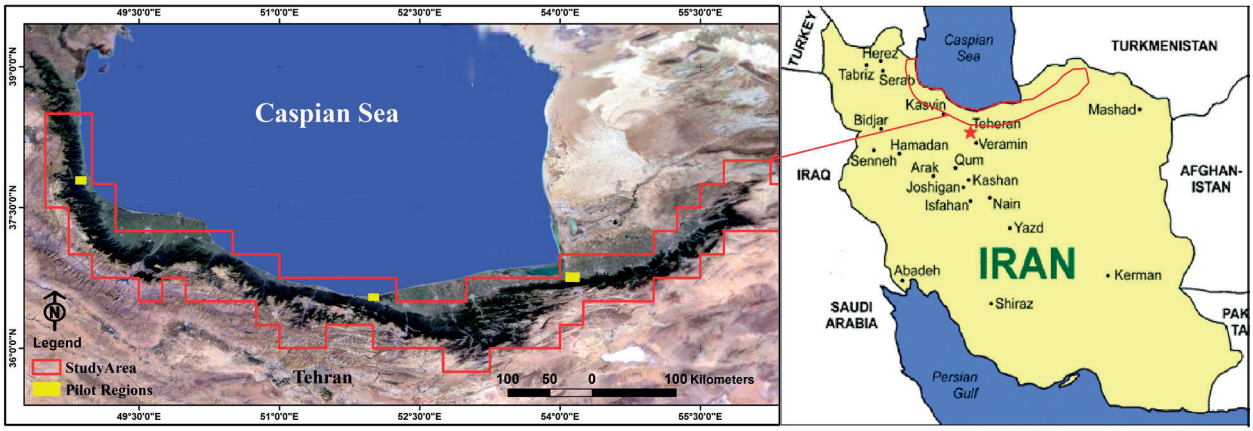

Fig. 1. Location of the study area in the north of Iran (source: Google)

Table 1. Definition of land cover classes for Hyrcanian forests data set

Land cover		Definition
Forest	dense	tree canopy cover > 50%
	semi-dense	50% > tree canopy cover > 25%
	sparse	25% > tree canopy cover > 5%
Orchard		trees of stone fruits and citrus, tea shrubs
Non-forest		covered by bushes, shrubs, grasses, crops, rock and bare soil, urban area, water bodies

each test was estimated from all pixels not used as training data. Table 1 shows land cover classes in Hyrcanian forests used for classification. It is worth saying that the forest density classes in Table 1 were selected based on internal guidelines of Forests, Range and Watershed Management Organization of Iran.

Training and accuracy samples selection. Training data selection is one of the major factors determining to what degree the classification rules can be generalized to unseen samples (Paola, Schowengerdt 1995). This factor could be more important for obtaining accurate classifications than the selection of classifiers. Many studies have demonstrated the training constants options, such as kernel type and gamma in case of SVM (Huang et al. 2002; Melganni, Bruzzone 2004; Pal, Mather 2005; Mountrakis et al. 2011; Yang, Ross 2012). For polynomial kernels better accuracies were achieved on data with three input variables as the polynomial order *P* increased from 1 to 8, suggesting the need for using high-order polynomial kernels when the input data have very few variables (Huang et al. 2002). For radial basis function (RBF) kernels the accuracy increased slightly when γ increased from 1 to 7.5. No obvious trend of improvement was observed when γ increased from 5 to 20. An experiment using arbitrary data points revealed that the misclassification error is a function of γ (Huang et al. 2002).

In the current study, according to Huang et al. (2002), 10% of pilot region pixels were selected as training and accuracy samples (Table 2). The training and accuracy samples were approximately 80 and 20% of the total samples, respectively. Accuracy assessment was performed using RBF kernels (γ = 7.5) and accuracy samples.

Classification and accuracy assessment method of the pilot regions. Land cover maps of three pilot regions (Kordkuy: eastern Hyrcanian range, Noor: central Hyrcanian range and Talesh: western Hyrcanian range) were classified using supervised classification by means of nine classifiers of SVM, ML, NN, minimum distance to mean (MiD), parallelepiped (P), Mahalanobis distance (MaD), spectral angle mapper (SAM), spectral information divergence (SID) and binary encoding (BE). The accuracies of land cover maps were assessed by 1,426 accuracy samples (pixel) using overall accuracy (OA) and Kappa coefficient (Richards 2013).

The total results were ranked based on their OA and Kappa coefficient values, which resulted in the final choice of SVM for the subsequent analyses (Table 3).

As such, the SVM classifier returned the highest rate of average Kappa coefficient of 0.94 compared to other classifiers, which justified its further use for the large-area classification.

Classification method of study area. According to results of pilot regions in the Hyrcanian forests, the images of the study area were classified using the supervised classification method and SVM classifier, for which the classes included sparse, semi-dense and dense forest canopy cover, as well as orchard and non-forest classes (Table 1). Then land cover maps were extracted.

Sampling design of study area. Many sample designs are possible using a sample survey framework (Cochran 1977; Lohr 1999) and here we focus on strategies that apply to obtaining field measurements for accuracy assessment. The large-area accuracy assessments of land cover map often employ two-stage sampling (Edwards et al. 1998; Nusser, Klaas 2003). This sampling

Table 2. Number of training and accuracy samples (pixels) in pilot regions

Pilot region	Land cover	Training sample	Accuracy sample	Total
Talesh	forest	942	234	1,176
	orchard	602	151	753
	non-forest	552	138	690
Noor	forest	813	203	1,016
	orchard	516	129	645
	non-forest	433	108	541
Kordkuy	forest	764	191	955
	orchard	522	130	652
	non-forest	471	118	589
Total		5,615	1,426	7,041

Table 3. Overall accuracy (OA) and Kappa coefficient of different classifiers of the pilot regions

Region	Coefficient	Classifier								
		BE	SID	P	SAM	MiD	MaD	NN	ML	SVM
Talesh	OA (%)	59.01	93.95	83.20	89.37	96.56	95.35	97.59	97.35	99.18
	Kappa	0.164	0.757	0.540	0.646	0.865	0.795	0.907	0.899	0.969
Noor	OA (%)	37.37	81.43	30.02	81.21	81.64	85.10	86.61	81.64	95.03
	Kappa	0.103	0.663	0.048	0.674	0.675	0.734	0.742	0.688	0.909
Kordkuy	OA (%)	17.70	55.66	66.34	70.00	76.83	90.49	91.56	92.68	96.31
	Kappa	0.139	0.236	0.445	0.483	0.560	0.822	0.849	0.865	0.936
Average	OA (%)	38.03	77.01	59.85	80.19	85.01	90.31	91.92	90.56	96.84
	Kappa	0.135	0.552	0.344	0.601	0.700	0.784	0.833	0.817	0.938

BE – binary encoding, SID – spectral information divergence, P – parallelepiped, SAM – spectral angle mapper, MiD – minimum distance to mean, MaD – Mahalanobis distance, NN – neural network, ML – maximum likelihood, SVM – support vector machine

method was applied to establish a database of sample points as ground truth in the study area (6,024,554 ha).

At the first stage, the entire study area was divided into 93 primary sample units (PSUs) approximately 61,500 ha, based on the standard sheets of 1:50,000 scale topographic maps of NCC. Nevertheless, we ensured that all of PSUs covered roughly the same amount of study area. Following that, based on field visiting 14 PSUs (15%) were randomly selected for further sampling (Fig. 2). Individual pixels were selected from PSUs at the second stage of sampling. Resource constraints dictated sample size. The study team had a goal of field visiting about 1,800 points within the study area. We expected that access would be denied for approximately 10% of the sample points, indicating 2,000 sample points would be needed to achieve 1,800 responses.

According to this reason, at the second stage, a systematic grid of 2 × 2 km was designed and randomly overlaid on the selected PSUs. The intersections of the grids were considered as reference data points to assess the accuracy of the classified land cover map (Fig. 3). Table 4 shows the number of samples and measured samples in each PSU.

Accuracy assessment method of study area land cover map. In the majority of accuracy assessment applications, both the map and reference classifications are crisp and the descriptive accuracy analyses employ an error matrix to organize the data (Stehman 2009). Parameters such as overall, user's and producer's accuracies (OA, UA and PA) are used to summarize the error matrix information (Stehman 2009). However, we assessed the accuracies (OA, UA and PA) of land cover classes map using measured data samples (Table 5).

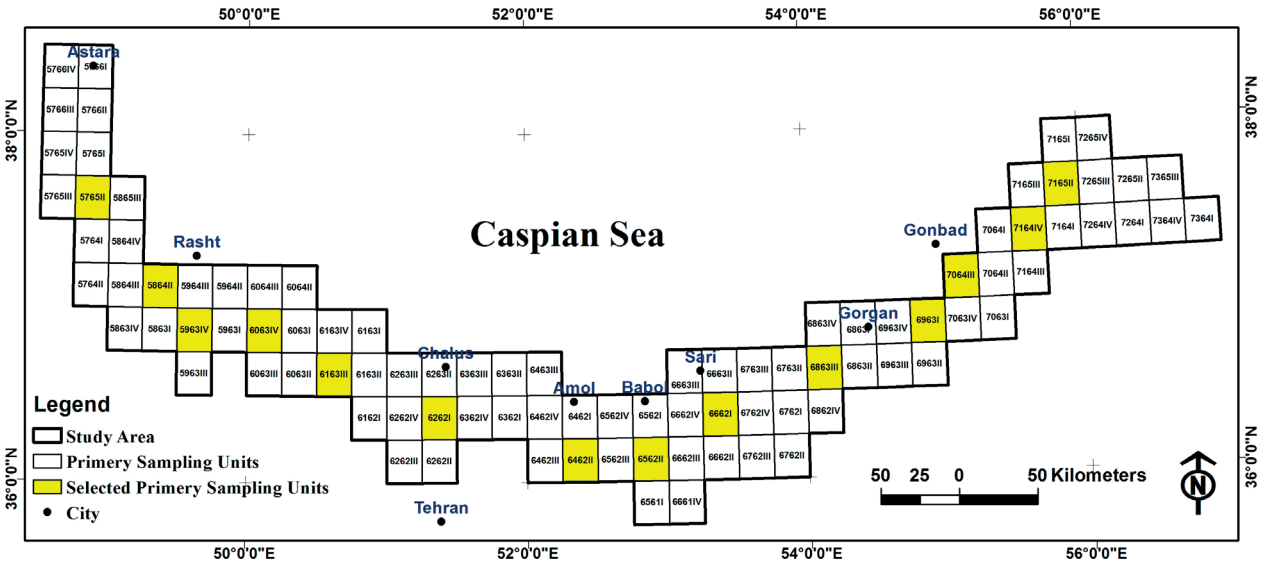

Fig. 2. Position of primary sample units (PSUs) and selected PSUs in the study area

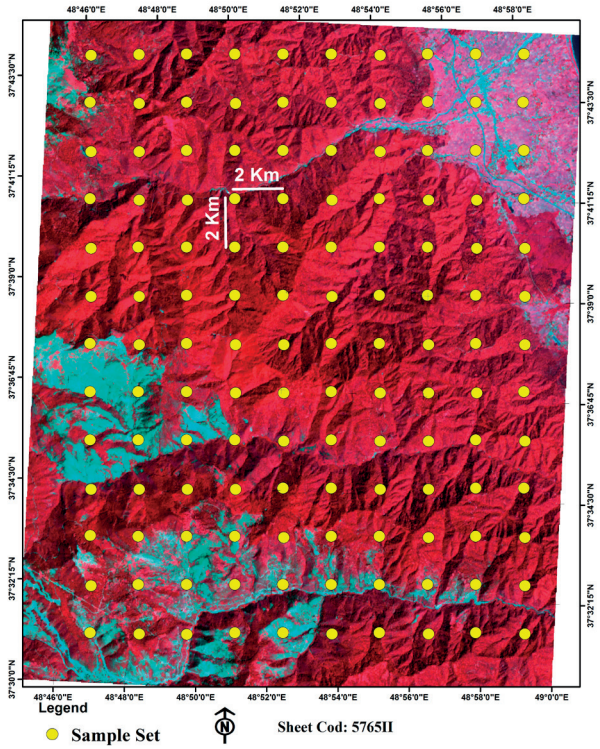

Fig. 3. Position of samples in primary sample unit 5765II

Table 4. Number of samples and measured ground truth samples in each primary sample unit (PSU)

PSU	No. of samples	No. of measured samples
5765II	130	124
5864II	142	132
5964IV	154	143
6063IV	142	127
6163III	154	138
6262I	140	128
6462II	130	126
6562II	154	144
6662I	140	127
6863III	140	128
6963I	142	135
7064II	130	123
7164IV	154	145
7165II	140	132
Total	2,007	1,852

Table 5. Number of measured ground control points (GCPs) in each land cover class

Land cover class	DF	SDF	SF	O	NF	Total
GCPs	404	377	237	92	742	1,852

DF – dense forest, SDF – semi-dense forest, SF – sparse forest, O – orchard, NF – non-forest

RESULTS

Validation

The previously described two-stage sampling method resulted in drawing 93 PSUs of the study area at the first stage, which in turn yielded a consequent number of 1,852 measured sample points in 14 PSUs across the land cover map of the Hyrcanian forests. These dense sample sets were homogenized and then applied for the final validation process of the classified Landsat 8 OLI images.

The accuracy assessment by 1,852 reference samples showed the overall accuracy and Kappa coefficient of 94.8% and 0.90, respectively (Table 6), i.e. the overall error of ± 5.2% for the classified map. In addition, the highest user's and producer's accuracies (ca. 100%) were achieved for non-forest and dense forest classes (Table 6).

Surface area of forest density classes, orchard and non-forest. The results of classified land cover map using the supervised classification method and SVM classifier also showed that the total surface areas of three dense, semi-dense and sparse forest classes accounted for 738,156, 599,439 and 312,903 ha, which corresponded to 45, 36 and 19% ratios of the total Hyrcanian forest area, respectively (Table 7). Based on the classification, the total surface area of Hyrcanian forests was thus calculated as 1,650,498 ha in summer 2014.

Table 6. Confusion matrix of the final classification for land cover classes map, overall accuracy = 94.8%, Kappa coefficient = 0.90

	DF	SDF	SF	O	NF	Total	UA
DF	**376**	21	5	0	0	402	93.5
SDF	25	**343**	15	1	0	384	89.3
SF	3	11	**213**	9	0	236	90.3
O	0	2	4	**82**	0	88	93.2
NF	0	0	0	0	**742**	742	100.0
Total	404	377	237	92	742	1,852	–
PA	93.1	91.0	89.9	89.1	100.0	93.1	–

DF – dense forest, SDF – semi-dense forest, SF – sparse forest, O – orchard, NF – non-forest, PA – producer's accuracy, UA – user's accuracy, number of accurate classified samples in bold

Table 7. Surface area of land cover classes in the Hyrcanian forests of Iran in 2014

	Non-forest	Orchard	Sparse forest	Semi-dense forest	Dense forest	Forest in total	Total
Area (ha)	4,259,873	114,183	312,903	599,439	738,156	1,650,498	6,024,554

Fig. 4 shows the distribution map of Hyrcanian forests density classes and non-forest in the north of Iran in summer 2014.

DISCUSSION

In this study, we consider the total surface area of the Hyrcanian forests of northern Iran using Landsat 8 OLI data. We obtained the 1,650,498 ha surface area for total sparse, semi-dense and dense Hyrcanian forests of Iran in summer 2014 (Table 7). Our results showed that the SVM classifier had the highest accuracy in the pilot regions (Table 3) followed by NN, ML, MaD, MiD, SAM, SID, P and BE, respectively. This result is in accordance with the results of Gualtieri and Cromp (1998), Huang et al. (2002), and Szuster et al. (2011).

Based on the accuracy assessment of the extracted land cover maps from Landsat 8 images in summer 2014, the overall accuracy and Kappa coefficient were 94.8 and 0.90, respectively (Table 6), which represented the overall error of ± 5.2% that would be an acceptable estimated error. It is worth saying that the overall accuracies in the previous studies on the same study area using ML classifier were about 80 and 96% for 2003 and 2008, respectively (Mirakhorlou 2003; Mirakhorlou, Akhavan 2008). Salman Mahini et al. (2012), who extracted an eastern Hyrcanian forest map using the classification method and ML classifier on Landsat ETM+ images in 2010, obtained the overall accuracy and Kappa coefficient of 91% and 0.70, respectively. Rezaee et al. (2008) classified Landsat ETM+ derived forest/non-forest maps of Arasbaran forest (northwestern Iran) using SVM classifier, and reported the overall accuracy and Kappa coefficient of 97% and 0.96, respectively. A further example was Tazeh et al. (2014), who used Landsat ETM+ images and reported 0.94 and 98% above-mentioned accuracy diagnostics. Their study also revealed 100% user's accuracy of forest class that showed the ability of Landsat images to detect forest from other land cover classes. The status quo literature generally suggests the ability of Landsat imagery for thematic mapping of attributes such as forest density, which was also confirmed by our findings on a larger spatial scale and by applying a substantially higher number of validation samples than those from the literatures.

One of the advantages of SVM classifier is to enable accurate mapping by the simultaneous use of a reference sample as training and validation samples (i.e. jacknifing). Our results showed no overlap between non-forest (i.e. agriculture, residential, pasture, bareland and water) and forest density classes by returning 100% user's accuracy. One may also note the heterogeneities existing within the orchards across the large geographic area of this study. The orchards in the low elevation forests (100–700 m a.s.l.) of the Hyrcanian forests comprise stone fruits in the eastern part, citrus trees in central part and tea and tobacco in the western part, which are occasionally associated with similar spectral reflectance as semi-dense and sparse forests. This was one of the factors that presumably had a negative impact on classification accuracy, with an example being the reduction of producer's accuracy from 93.1% in dense forest to 89.1% in orchard class (Table 6). Nevertheless, the dense forest

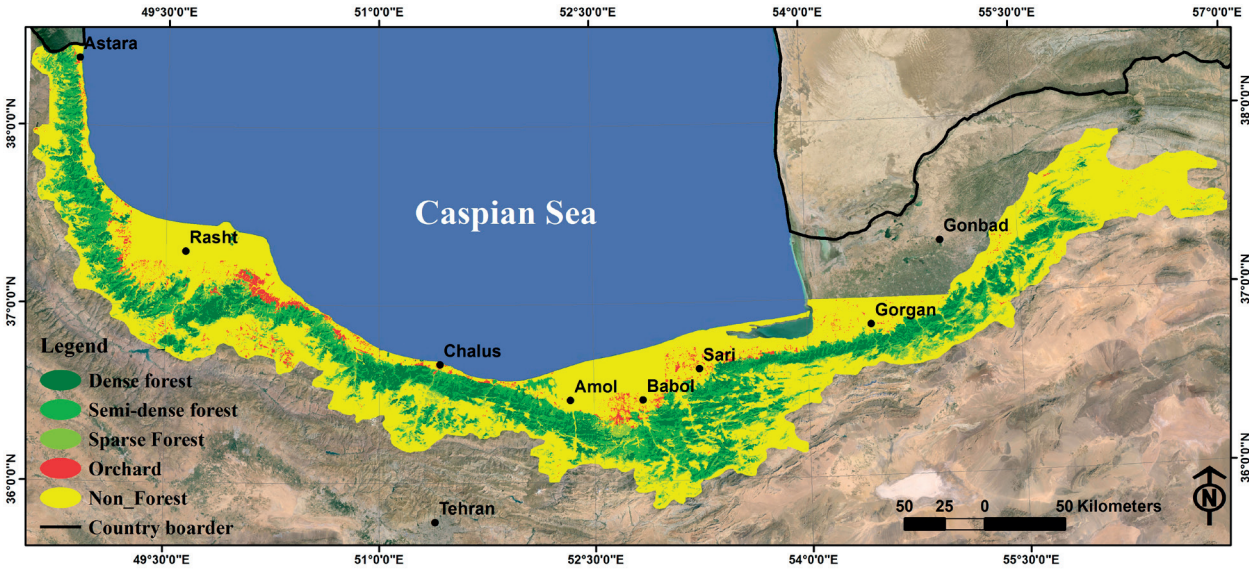

Fig. 4. Hyrcanian forest density classes and non-forest map extracted from Landsat 8 Images in 2014

class did not show any spectral reflectance overlap with the orchard class due to its substantially denser crown cover compared to that of the orchard class. Therefore, the classification of dense forest class was accomplished with a higher accuracy than both semi-dense and sparse forest classes. Of further importance was also the dense class, which was located in the middle (700–1,800 m a.s.l.) and high (1,800–2,200 m a.s.l.) altitudinal range of the Hyrcanian forests, occurring where no orchards exist, while orchards are commonly established in the vicinity of semi-dense and sparse forests.

CONCLUSIONS

One of the main problems in the mapping of our Hyrcanian forests in Iran is the interference of forests with orchards. The results of this study showed that SVM is the best classifier to separate forests from orchards as well as to classify forest density classes. Furthermore, the results of this study generally refuse using common parametric classifiers for forest area mapping, which are currently applied in practical forest inventory in northern Iran. On the contrary, our precisely large-scale mapped results of Hyrcanian forests in 2014 can be further applied to many other studies such as forest carbon cycle, ecological restoration and forest planning and management. We thus further suggest our framework to be used in decision-making processes as well as for surveys on national and regional planning (e.g. conservation, restoration and development) in the Hyrcanian forests.

Acknowledgment

We thank M. Amin Amlashi, R.A. Khorrami, and S. Yousefi for assistance with field work and data collection.

References

Akhavan R., Sagheb Talebi K., Zenner E.K., Safavimanesh F. (2012): Spatial patterns in different forest development stages of an intact old-growth Oriental beech forest in the Caspian region of Iran. European Journal of Forest Research, 131: 1355–1366.

Cochran W.G. (1977): Sampling Techniques. 3rd Ed. New York, John Wiley & Sons, Inc.: 428.

Dicks S.E., Lo T.H.C. (1990): Evaluation of thematic map accuracy in a land-use and land-cover mapping program. Photogrammetric Engineering and Remote Sensing, 56: 1247–1252.

Dixon B., Candade N. (2008): Multispectral land use classification using neural networks and support vector machines: One or the other, or both. International Journal of Remote Sensing, 29: 1185–1206.

Dube T., Mutanga O. (2015): Evaluating the utility of the medium-spatial resolution Landsat 8 multispectral sensors in quantifying aboveground biomass in uMgeni catchment, South Africa. ISPRS Journal of Photogrammetry and Remote Sensing, 101: 36–46.

Edwards T.C., Moisen G.G., Cutler D.R. (1998): Assessing map accuracy in a remotely sensed ecoregion-scale cover map. Remote Sensing of Environment, 63: 73–83.

Foody G.M., McCulloch M.B., Yates W.B. (1995): The effect of training set size and composition on artificial neural network classification. International Journal of Remote Sensing, 16: 1707–1723.

Gualtieri J.A., Cromp R.F. (1998): Support vector machines for hyperspectral remote sensing classification. In: Mericsko R.J. (ed.): Proceedings of the 27th AIPR Workshop: Advances in Computer Assisted Recognition, Washington, D.C., Oct 14–16, 1998: 221–232.

Huang C., Davis L.S., Townshend J.R.G. (2002): An assessment of support vector machines for land cover classification. International Journal of Remote Sensing, 23: 725–749.

Intergraph (2013): ERDAS Field Guide™. Huntsville, Intergraph Corporation Press: 792.

Jensen J.R. (2005): Introductory Digital Image Processing: A Remote Sensing Perspective. 3rd Ed. Upper Saddle River, Prentice Hall: 526.

Lohr S.L. (1999): Sampling: Design and Analysis. Pacific Grove, Brooks/Cole Publishing Company: 494.

Lu D., Weng Q. (2007): A survey of image classification methods and techniques for improving classification performance. Journal of Remote Sensing, 28: 823–870.

Melganni F., Bruzzone I. (2004): Classification of hyperspectral remote sensing images with support vector machines. IEEE Transactions on Geoscience and Remote Sensing, 42: 1177–1790.

Mirakhorlou K. (2003): Land use mapping of northern forests of Iran using Landsat 7 ETM+ data. Iranian Journal of Forest and Poplar Research, 11: 174–215. (in Persian with English abstract)

Mirakhorlou K., Akhavan R. (2008): Investigation on boundary changes of northern forests of Iran using remotely sensed data. Iranian Journal of Forest and Poplar Research, 16: 139–148. (in Persian with English abstract)

Mountrakis G., Im J., Ogole C. (2011): Support vector machine in remote sensing: A review. ISPRS Journal of Photogrammetry and Remote Sensing, 66: 247–259.

Nusser S.M., Klaas E.E. (2003): Survey methods for assessing land cover map accuracy. Environmental and Ecological Statistics, 10: 309–331.

Pal M., Mather P.M. (2005): Support vector machines for classification of in remote sensing. International Journal of Remote Sensing, 26: 1007–1011.

Paola J.D., Schowengerdt R.A. (1995): A review and analysis of backpropagation neural networks for classification of remotely sensed multi-spectral imagery. International Journal of Remote Sensing, 16: 3033–3058.

Qin Y., Xiao X., Dong J., Zhang G., Shimada M., Liu J., Li C., Kou W., Moore B. (2015): Forest cover map of China in 2010 from multiple approaches data sources: PALSAR, Landsat, NODIS, FRA and NFI. ISPRS Journal of Photogrammetry and Remote Sensing, 109: 1–16.

Rezaee M.B., Rostamzadeh H., Feyzizade B. (2008): Evaluating of forest change detection using RS and GIS. Iranian Journal of Geographical Researches, 62: 143–159. (in Persian with English abstract)

Richards J.A. (2013): Remote Sensing Digital Image Analysis. 5th Ed. Berlin, Heidelberg, Springer-Verlag: 494.

Saadat H., Adamowski J., Bonnell R., Sharifi F., Namdar M., Ale-Ebrahim S. (2011): Land use and land cover classification over a large area in Iran based on single date analysis of satellite imagery. ISPRS Journal of Photogrammetry and Remote Sensing, 66: 608–619.

Salman Mahini A., Nadali A., Feghhi J., Riyazi B. (2012): Classification of Golestan province of forest areas by maximum likelihood algorithm using Landsat 7 ETM+ data. Iranian Journal of Environmental Science and Technology, 14: 57–72. (in Persian with English abstract)

Stehman S.V. (1992): Comparison of systematic and random sampling for estimating the accuracy of maps generated from remotely sensed data. Photogrammetric Engineering and Remote Sensing, 58: 1343–1350.

Stehman S.V. (2009): Sampling designs for accuracy assessment of land cover. International Journal of Remote Sensing, 30: 5243–5272.

Szuster B.W., Chen Q., Borger M. (2011): A comparison of classification techniques to support land cover and land use analysis in tropical coastal zones. Applied Geography, 31: 525–532.

Tazeh M., Ghezelsaflou N., Sadeghi A.M. (2014): Evaluating capability of Landsat satellite images for forest mapping. In: Karkeabadi Z. (ed.): Proceedings of the 1st National Conference of Geography, Urban and Development, Tehran, Feb 27, 2014: 1518–1530. (in Persian with English abstract)

Yang S., Ross S.L. (2012): Comparison of support vector machine, neural network and CART algorithms for the land-cover classification using limited training data points. ISPRS Journal of Photogrammetry and Remote Sensing, 70: 78–87.

Received for publication January 30, 2017
Accepted after corrections June 20, 2017